Estuarine, Coastal and Shelf Science 285 (2023) 108308

Contents lists available at ScienceDirect

Estuarine, Coastal and Shelf Science

journal homepage: www.elsevier.com/locate/ecss

Space–time analyses of sediment composition reveals synchronized dynamics at all intertidal flats in the Dutch Wadden Sea

Eelke O. Folmer [a,*], Allert I. Bijleveld [b], Sander Holthuijsen [b], Jaap van der Meer [b,c,d], Theunis Piersma [b,e], Henk W. van der Veer [b]

[a] Ecospace, Ecological Research and Environmental Informatics, Lemmer, The Netherlands
[b] NIOZ, Royal Netherlands Institute for Sea Research, Department of Coastal Systems, The Netherlands
[c] Vrije Universiteit Amsterdam, Department of Ecological Science, Amsterdam, The Netherlands
[d] Wageningen Marine Research, Den Helder, The Netherlands
[e] Conservation Ecology Group, Groningen Institute for Evolutionary Life Sciences (GELIFES), University of Groningen, Groningen, The Netherlands

ARTICLE INFO

Dataset link: https://figshare.com/articles/software/Script_and_background_data_for_ECSS_sediment_paper/21997148/1

Keywords:
Intertidal flats
Sediment
Wadden Sea
Hydrodynamics
Spatial panel models

ABSTRACT

Intertidal mudflat systems are shaped by geological processes and an interplay of hydrodynamics, sediment availability and ecological processes. All around the world these systems are affected by relative sea level rise (RSLR), changing climate and by human activities such as sediment nourishments, dredging, hydrological engineering and bottom trawling. These kinds of perturbations cause changes in morphology and sediment composition which may cause shifts in the composition, spatial distribution and productivity of benthic communities. We analysed the spatial and temporal variability of the sediment grain size of more than 900 km^2 intertidal flats in the Dutch Wadden Sea in the period 2009–2019. The large scale coverage was achieved by yearly grid sampling at more than 4000 stations. Spatial panel data models were used to analyse changes in median grain size and mud content between years and to estimate the effects of resuspension due to wind and the accumulation of silt during summer. We show that between years the sediments of the intertidal flats changed synchronously throughout the study area and that the flats became coarser during the period 2011–2015 and muddier again between 2015 and 2019. The system wide changes and the absence of clear local deviations leads to the hypothesis that a large scale factor like changing hydrodynamic regime (e.g. due to RSLR), variability in the composition of suspended sediment in the North Sea or changing microphytobenthic productivity were causally involved in the coarsening of intertidal flats. Our data and analysis provides a base for further scientific enquiry but longer time series on higher temporal resolution of both sediment data and the physical and ecological environment are required. Models simulating the environment may provide further insight into possible development of sediment composition of the intertidal flats of the Wadden Sea.

1. Introduction

How tidal flats and adjoining saltmarshes are shaped and how sediments respond to natural and human induced conditions has inspired generations of geomorphologists, engineers and ecologists. These questions are increasingly important in the face of sea level rise because of the protection that soft sediment tidal ecosystems offer against floodings (Borsje et al., 2011; Temmerman et al., 2013). Tidal flats attenuate waves and they retain sediments which enable tidal flats and adjoining marsh systems to grow and keep up with sea level rise (Cahoon et al., 2006; Kirwan and Megonigal, 2013). The morphology and sediment grain size control the physical, chemical and ecological conditions and when this changes, intertidal ecosystems also change in terms of nutrient cycling, benthic primary production, the distribution of organisms and foodweb dynamics (e.g. Herman et al., 2001; Compton et al., 2013a). In their turn, organisms and ecological processes may also affect the morphology and sediment grain size of intertidal mudflat systems (Widdows and Brinsley, 2002; Widdows et al., 2004; Mullan Crain and Bertness, 2006; Montserrat et al., 2008). Knowledge of intertidal mudflat systems and sediment dynamics is essential for understanding and modelling the impacts of e.g. sea level rise, wind climate, sediment nourishments, dredging and bottom trawling.

Understanding intertidal systems and sediment dynamics is challenging because of the interplay of many known and unknown geological, geomorphological, hydrodynamical, and ecological processes acting across multiple spatial and temporal scales (Roberts et al., 2000;

* Corresponding author.
E-mail address: eelke@ecospace.io (E.O. Folmer).

https://doi.org/10.1016/j.ecss.2023.108308
Received 20 September 2022; Received in revised form 8 February 2023; Accepted 17 March 2023
Available online 23 March 2023

Wang et al., 2012). On large scales, the geological setting, sea level variations, tides, and sediment availability determine the morphological development and sediment distributions. On smaller scales, interactions between hydrodynamics and sedimentation/erosion processes shape the intertidal systems (Roberts et al., 2000; Janssen-Stelder, 2000; Friedrichs, 2011; Wang et al., 2012). Tidal flow velocity and orbital velocity are attenuated across intertidal flats leading to a decreasing bottom shear stress gradient in the tidal propagation direction (Le Hir et al., 2000). The sediment composition of the intertidal flats depends on the balance between bottom shear stress that causes erosion and the erodability properties of the sediment and sediment settling rates. Fine sediments tend to settle only under calm conditions, while coarse sediments also settle under rough conditions (Grabowski et al., 2011). Settling of fine sediment is stimulated by organic matter which reinforces flocculation processes (van Straaten and Kuenen, 1958; Eisma, 1986). The erodability of sediment depends on particle size distributions (composition), its cohesion and adhesion properties and the concentration of extracellular polymeric substances excreted by diatoms (Paterson and Black, 1999; Herman et al., 2001; Grabowski et al., 2011). We refer to Grabowski et al. (2011) for a comprehensive review about erodability of sediments. The combination of these processes leads to spatial repartitioning patterns where the sediments near the borders of intertidal flats are generally coarse and the sediments near the marshes and tidal divides are fine-grained.

Under constant long-term conditions the morphology and sediment composition of an intertidal mudflat system would develop towards a dynamic equilibrium. Intertidal mudflat systems, however, are never in equilibrium due to a.o. tides, changing weather, seasonal variability, the 18.6 year nodal cycle (Oost et al., 1993), biological processes, and their interactions causing spatio-temporal variability in the erosion and deposition processes. For example, seasonal variability in hydrodynamic conditions and biological activity lead to seasonal variability in deposition and erosion leading to seasonal variability in the sediment composition of intertidal flats (Kamps, 1962; Herman et al., 2001). In the Wadden Sea fine sediments accumulate during summer when strong winds are sporadic and the production of extracellular polymeric substances by microphytobenthos – i.e. unicellular eukaryotic algae and cyanobacteria that grow in the upper few millimeters of intertidal flats – is high (Widdows et al., 2004; Zwarts et al., 2004). In autumn and winter when the winds are strong and the biological activity is low, the accumulated fine sediments tend to resuspend and remain in suspension longer than in summer. In similar vein as Roberts et al. (2000) and Friedrichs (2011), we define the dynamic equilibrium as the long-term state where sediment composition is relatively constant. In the case of a dynamic equilibrium, only large-scale perturbations will have detectable effects on the sediment composition. Examples of large-scale factors that may perturb the dynamic equilibrium when they change, are sea level, hydrodynamic climate and the composition of the supplied sediment (van Straaten and Kuenen, 1958; Oost, 1995; Malvarez et al., 2001; Van Goor et al., 2003). However, our current knowledge about these known and unknown processes is too limited to assess their impacts on intertidal systems (Wang et al., 2012).

The purpose of this paper is to analyse the spatio-temporal development of grain size distributions of intertidal flats in the Dutch Wadden Sea to improve our understanding of how intertidal flats respond to changing conditions. This requires long-term and large-scale data about sediment composition. Up until the large-scale Synoptic Intertidal Benthic Surveys (SIBES) (Bijleveld et al., 2012; Compton et al., 2013a) – an annual monitoring program covering all intertidal flats of the Dutch Wadden Sea – was in place, such data did not exist. We analysed the sediment composition over the period 2009–2019 and reveal spatially synchronous changes in sediment composition suggesting that one or more large scale factors cause the changes.

2. Methods

2.1. Study area

The Wadden Sea is located in the south-eastern coastal zone of the North Sea and borders Denmark, Germany and the Netherlands (Fig. 1). The surface sediments of the south-eastern North Sea consist mainly of sand and muddy sand (Schlüter and Jerosch, 2009). The Wadden Sea started emerging after the last glacial period approximately 7000 years ago during a period of reduced sea level rise. During this period sediments from the North Sea were transported to the coastal plains and the Wadden Sea area (Beets and Spek, 2000). The current sediment composition and distribution are largely the outcome of the supply and sorting processes since the period that the Wadden Sea emerged. The area now consists of saltmarshes, intertidal flats, shallow subtidal flats, drainage gullies and deeper inlets and channels (van Straaten and Kuenen, 1958; Oost, 1995). It is the largest coherent system of intertidal flats in the world and it was designated an UNESCO World Heritage site because of its 'universally outstanding natural values'. These natural values are mainly based on the scale of the largely unbounded geomorphological and ecological processes that characterize the area (Reise et al., 2010).

In the Dutch part of the Wadden Sea tidal amplitudes range from west to east between 1.5 and 3.0 m (Dijkema et al., 1980). Tidal currents and exposure to waves strongly differ between regions due to differences in tidal range, geomorphology, fetch and the occurrence of barrier islands (Dijkema et al., 1980; Donker, 2015; Folmer et al., 2016). The geomorphology and sediment composition are strongly influenced by tidal currents and wind-driven waves (Wang et al., 2012). Tidal flat areas that border large water bodies or wide gullies are exposed to waves and currents and therefore consist of coarse sands. In sheltered areas such as inside the Ems-Dollard estuary (Fig. 1: TB30) and at the shores and tidal divides the fractions of fine-grained particles are high (Fig. 3) (van Straaten and Kuenen, 1958). The numbers, biomass and diversity of macrozoobenthos increase from exposed towards sheltered tidal flats (Compton et al., 2013a).

The Wadden Sea and its hinterland are threatened by relative sea level rise and under the expected long term rates it is unlikely that natural sedimentation will be sufficient to compensate for it (Kabat et al., 2009; Wang et al., 2012). The rate of sea level rise along the coast of the Netherlands was relatively constant between 1890 and 2014 and amounts to approximately 1.9 mm y^{-1}. In the Dutch Wadden Sea, gauge measurements at four different stations show average rates of sea level rise between 1.3 and 2.0 mm y^{-1} (Vermeersen et al., 2018; Fig. 2). Analyses of bathymetries over the period 1927/1935-2005 show that a total of 572.5 million m^3 sediment was imported to the Wadden Sea (excluding the Ems-Dollard, TB30) which was more than required to compensate for sea level rise (Wang et al., 2012; Elias et al., 2012). Most of the sediment deposition took place in the channels in the Western Wadden Sea (TB39 and TB37), probably in response to the closure of the Zuiderzee (Elias et al., 2012; Colina Alonso et al., 2021). In general the erosion and deposition were more subtle on the tidal flats than in the gullies. On the tidal flats most of the deposition took place along the main land Frisian coast in TB37 (Fig. 1) (Elias et al., 2012).

2.2. Field sampling and laboratory analysis

The entire intertidal Dutch Wadden Sea was sampled every year between 2009 and 2019. Samples were taken on a 500 m grid and on randomly located stations within the grid to improve the fine-scale accuracy of spatial interpolations (Bijleveld et al., 2012). Between 4051 and 4246 samples were collected and analysed every year, which made a total of 45 808 over the study period (Table 1). Most of the sampling took place in the months between June and August but in 2009 the sampling program ran until mid October. The stations were not sampled

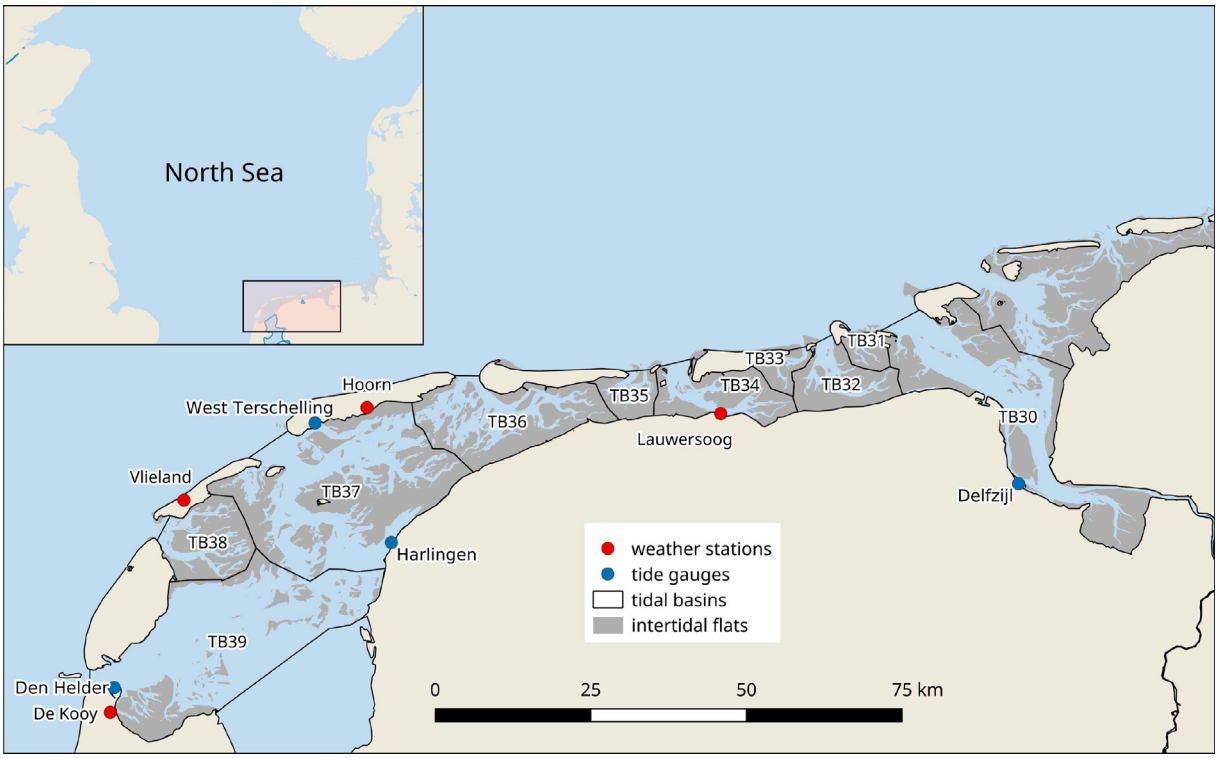

Fig. 1. The Dutch Wadden Sea with its intertidal flats and tidal basins. The tidal basins are labelled TB30-TB39. The locations and names of the weather stations and tidal gauges are included. The eastern part of TB30 is in Germany and is not included in this study.

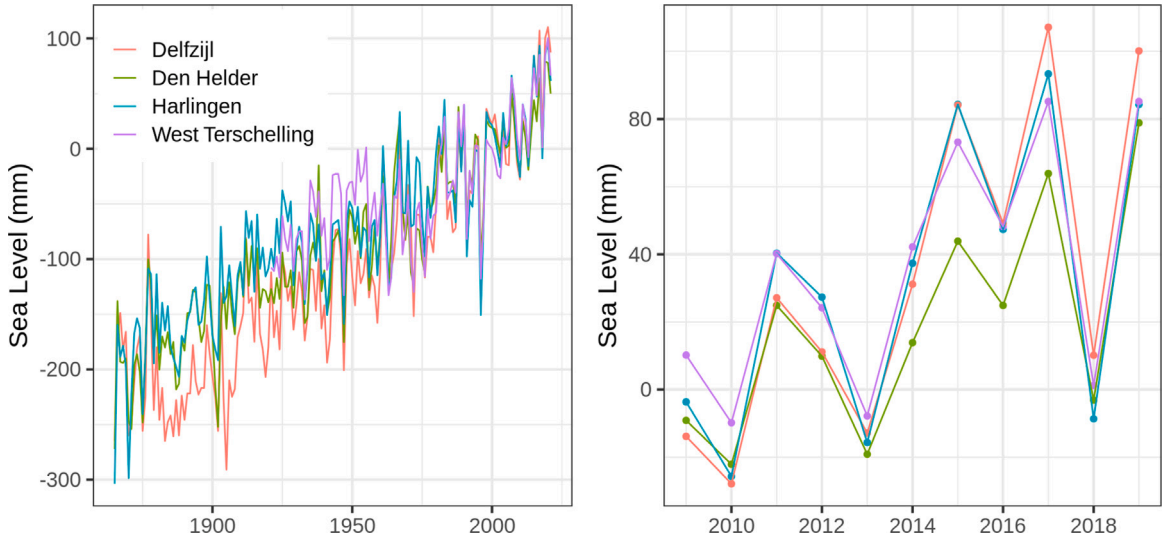

Fig. 2. Yearly mean sea levels at four tide-gauges in the Dutch Wadden Sea during the period 1865–2021. The right panel shows the sea levels during the years 2009–2019 in detail. In similar vein as Vermeersen et al. (2018), the site-level means of the years 1991–2016 have been removed. Data were obtained from the Permanent Service for Mean Sea Level; levels obtained from this service are corrected for vertical land motion (Holgate et al., 2013).

at the same dates across years. Supplement A shows when and where sampling took place.

Sampling stations were visited by foot during low tide and by boat during high tide. Sediment samples were taken with a small core with a diameter of 33 mm from the surface of the intertidal flats to a depth of 4 cm and then frozen at −20 °C. In the laboratory, the samples were freeze-dried for up to 96 h and then homogenized with a mortar and pestle. Homogenized samples were weighed and placed into 13 ml polypropylene auto-sampler tubes with degassed water that was purified by means of reverse osmosis. Grain size distributions were measured with a particle size analyser which uses laser diffraction and Polarization Intensity Differential Scattering technology (Coulter LS 13 320, optical module 'grey'). It measures grain sizes from 0.04 to 2000 μm in 126 size classes. It is important to note that our samples were not treated with hydrogen chloride and hydrogen peroxide to remove calcium and organic material. All samples were collected, treated and analysed using the same protocols and instruments. In fact, 80%–90% of the samples were treated and measured by the same laboratory technician. In the Dutch intertidal the fraction of particles $< 16\,\mu m$ in untreated samples is approximately twice as large as in samples from which calcium and organic material has been removed. Regression analysis shows that the R^2 of the relationship between the $< 16\,\mu m$

Table 1
Number of sediment samples taken per year in the tidal basins of the Dutch Wadden Sea.

Tidal Basin	2009	2010	2011	2012	2013	2014	2015	2016	2017	2018	2019
30 Eems-Dollard	407	400	365	383	381	385	414	420	406	415	428
31 Schild	90	77	86	84	85	89	87	84	82	82	85
32 Lauwers	299	293	285	258	263	279	283	287	259	278	289
33 Eilanderbalg	97	94	92	94	86	105	101	105	96	98	99
34 Zoutkamperlaag	402	408	407	402	353	330	328	336	339	334	334
35 Pinkegat	214	223	218	216	201	160	162	156	165	165	152
36 Borndiep	654	656	644	639	640	633	627	619	637	624	631
37 Vlie	1188	1212	1187	1149	1187	1284	1260	1284	1235	1268	1281
38 Eijerlandse Gat	393	389	377	401	380	406	398	407	407	404	416
39 Marsdiep	468	487	486	481	475	511	513	420	525	514	531
Total	4212	4239	4147	4107	4051	4182	4173	4118	4151	4182	4246

fractions of treated and untreated samples is very large (Zwarts et al., 2004) which implies that our results probably generalize to treated samples. For further details concerning sediment analysis we refer to Compton et al. (2013b).

The composition of samples can be characterized by means of full grain size distributions for which different summarizing statistics can be used. Zwarts et al. (2004) showed that commonly used statistics of sediment grain size are highly correlated for the intertidal flats in the Wadden Sea. We analysed the median grain size (*mgs*, μm) and the mud content (*mud*, %). Mud is defined as a percentage of the volume of the particles between 0.04 and 63.00 μm of all particles. The median grain size is an effective descriptor of the distribution when mud contents are relatively low (< 5%–10%). The mud content is an effective statistic to detect possible impacts of perturbations which mainly affect fine sediment particles.

2.3. Data handling

Before formal analyses we provide insight into the data by means of maps of the mean, standard deviation and average yearly changes of *mgs* and *mud*. Prior to plotting and analysis, the original point data from the 500 m grid were spatially aggregated by computing for each cell of a 750 m × 750 m grid, the yearly mean values of *mgs* and *mud*. Spatial aggregation helps to avoid possible missing observations in the 500 m grid which is required for spatial panel data models. Particularly, not 100% of the locations were visited every year and there were randomly located points inbetween the regular grid points. Over the years, in the 750 m grid consisting of a total of 2205 cells, ~4% of the cells enclosed between 5–8 stations, ~8% of the cells enclosed 4 stations; ~13% enclosed 3 stations; ~34% enclosed 2 stations; and ~40% enclosed 1 station. By selecting the cells that enclosed 1 or more stations each year, we obtained a fully balanced dataset with a cross-sectional dimension of 1619 individual cells and a longitudinal dimension of 11 years.

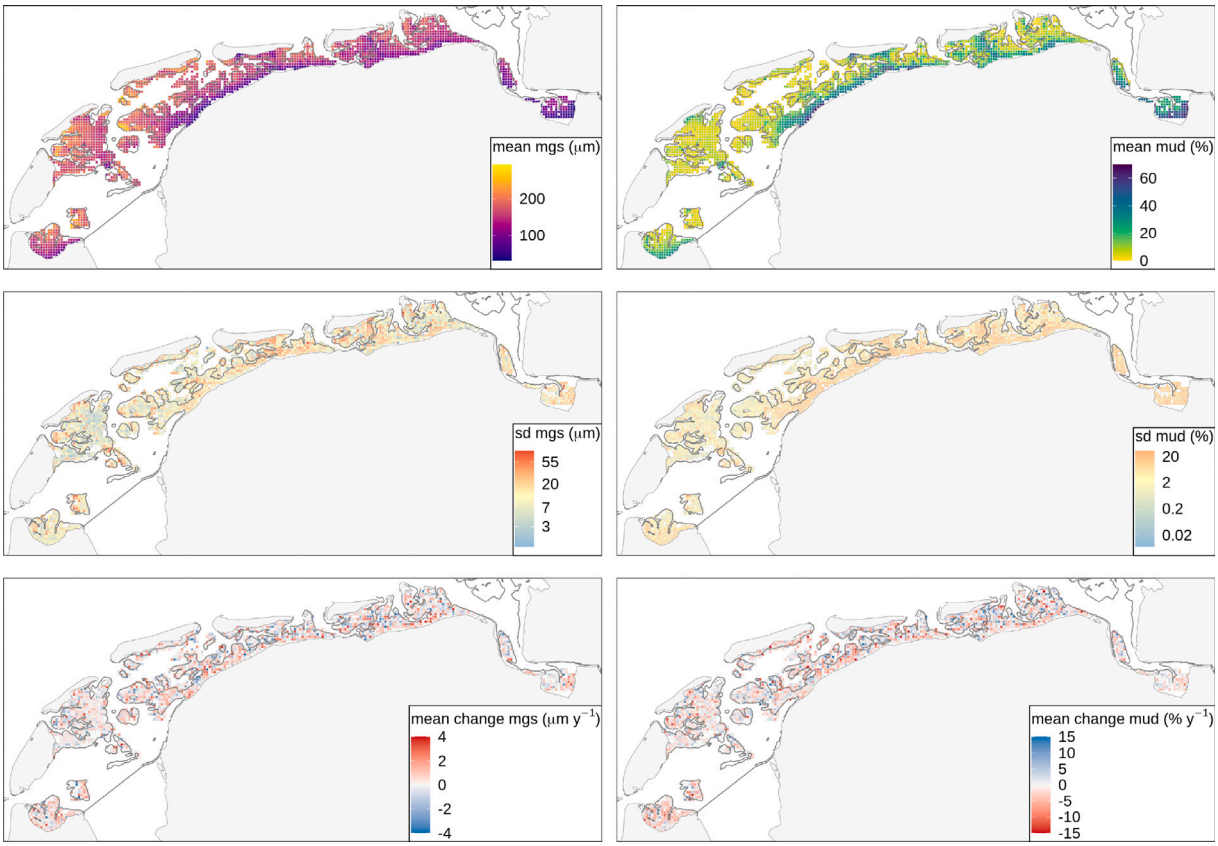

Fig. 3. Mean, standard deviation (sd) and mean yearly change of *mgs* and *mud* over the period 2009–2019. The mean changes in *mgs* are the slopes of the simple linear regression models with year as linear predictor. In the case of *mud*, the regression coefficients are based on the logit-transformed mud concentrations ($Amud_{i,t} = logit(mud_{i,t}) - \overline{logit(mud_i)}$). In the map the yearly percentage change ($100 \cdot (e^{\beta} - 1)$) is represented.

For each 750 m × 750 m grid cell the yearly *mgs* and *mud* anomalies were computed. We analyse anomalies rather than measured values because there is systematic spatial pattern in the measured values related to the average hydrodynamic regime (Donker, 2015; Folmer et al., 2016; Gräwe U. Flöser et al., 2016). By analysing anomalies we control for spatially variant and temporally invariant variables and thus focus on temporally variable factors. The *mgs* anomalies were computed by subtracting from each yearly cell value the mean over all years, i.e. $Amgs_{i,t} = mgs_{i,t} - \overline{mgs_i}$ (i is an index for cell and t is an index for year). The distribution of *mud* is right skewed because many areas have very low values while the muddy areas show large variation in mud content (Supplement B, Figure S2). Therefore, the *mud* anomalies were defined as the difference between the logit-transformed mud fractions (volume percentage/100%) of the yearly grid values and the means of the logit-transformed mud fractions over all years, i.e. $Amud_{i,t} = logit(mud_{i,t}) - \overline{logit(mud_i)}$. To avoid taking the log of zero we added 0.01 to each value $mud_{i,t}$. To illustrate the differences in mud concentration between years on a non-transformed scale (Fig. 5), we also calculated the anomalies by subtracting the gridcell level means from each observation, i.e. $Amud0_{i,t} = mud_{i,t} - \overline{mud_i}$.

For all cells with more than 5 observations (2066 out of 2205) we computed the average change of *Amgs* and *Amud* over the years by means of a simple linear regression model with year as linear predictor. Because the data and the regression coefficients were spatially autocorrelated these models were not used for statistical inference.

Wind waves have large influence on the morphology and sediment composition in shallow intertidal areas and the processes underlying bottom shear stress causing erosion and resuspension are very complex. How wind waves form and cause shear and erosion at intertidal flats depends on the interaction between wind characteristics (speed, direction and duration), fetch length, tidal elevation, tidal currents, the elevation and slope of the intertidal flats, sediment composition and the density of microphytobenthos and other benthos (Mariotti et al., 2010; Grabowski et al., 2011). The only way in which high resolution data about the effects of wind and shear on intertidal flats can be estimated realistically is by means of hydrodynamic models which integrate the essential processes and information. This type of hydrodynamic modelling is an active field of research but accurate information on high temporal resolution is not available for the Dutch Wadden Sea. To investigate and account for the effects of wind on *Amgs* and *Amud* we made use of hourly wind measurements from different weather stations in the Dutch Wadden Sea area. Wind data were obtained from the Dutch national weather service (www.knmi.nl) for four weather stations: De Kooy, Hoorn Terschelling, Vlieland and Lauwersoog (Fig. 1). The wind velocities (ms^{-1}) and directions strongly correlate between stations but there are slight systematic differences in the average wind velocities (supplement C). The cells in which sediment was sampled were matched with the weather stations on the basis of the shortest straight line distance. Observations for station Vlieland between 2 July 2015 and 3 August 2015 were missing. Missing observations were imputed by fitting a linear regression model with response variable wind velocity at Vlieland as a function of the wind velocity at the nearest station Hoorn (Fig. 1) with the pairwise complete data for the months June–October between 1 June 2009 and 29 October 2016. The regression model (with intercept 1.14 and slope 1.06 and $R^2 = 0.78$) was used to predict the missing values for Vlieland on the basis of the measurements at Hoorn; prediction error was ignored.

2.4. Modelling approach

The objective of our modelling approach was to analyse the change in grain size between years while accommodating for the possible effects of resuspension due to wind and the accumulation of silt during summer. We used non-spatial models, simultaneous autoregressive models and spatial panel error models. We analysed the effect of wind on *Amgs* and *Amud* over short- (days) and long timescales (months). Christiansen et al. (2006) showed that during summer, a mobile toplayer may be resuspended and redeposited leading to variability in bed level and grain size on the timescale of days. For the short-term wind effect we included as a predictor variable the sum of the hourly wind velocities greater than 5 ms^{-1} during 2 days prior to sampling ($wind_s$). Long-term effects of strong winds on bed level and grain size may vary substantially between systems and within systems; recovery times tend to range from weeks to months and after exceptional storms even up to years (Friedrichs, 2011; Yang et al., 2019; de Vet et al., 2020). The long-term wind predictor variable ($wind_l$) was computed as the sum of the weighted wind velocities greater than 8 ms^{-1} between 300-2 days prior to sampling. The wind speed values were down-weighted as a function of the number of days prior to sampling (dt) using a negative exponential function, $w(dt) = \frac{e^{-0.01 \cdot dt}}{\sum e^{-0.01 \cdot dt}}$. Seasonal dynamics in the deposition and erosion resistance, which is positively related the production and activity of phytoplankton and benthic diatoms is accounted for by including the number of days since 1 June as a predictor (*yday*). Because sampling stations were aggregated in a 750 m grid, the possibility of a difference in *yday* within a cell arose. Thanks to the fact that large mudflat areas are sampled in their entirety during single days, this did not occur.

We start by estimating a non-spatial linear regression model and test for spatial effects in the model residuals. The confirmation of spatial autocorrelation indicates a violation of the spatial independence assumption. We resolve the spatial dependence by estimating simultaneous autoregressive models for each year. Finally, we proceed with spatial panel error models to model spatial dependence and temporal change in a single model.

2.4.1. Non-spatial and spatial autoregressive models

We used a non-spatial linear regression model to explain yearly *Amgs* and *Amud* by $wind_s$, $wind_l$ and *yday* where year t and cell i are included as factors. For each year, we constructed scatterplots of the residuals against the mean residuals of the neighbouring cells (supplement D). The mean of the residuals of neighbouring cells was computed by multiplying the residual vector with the spatial weight matrix W. Cells within a cutoff distance of 2000 m are defined as neighbours. The spatial weights were row-normalized, i.e. each element of W was divided by the sum of its row elements such that the sum of each row equals 1. To remove residual spatial autocorrelation, we fitted simultaneous autoregressive models (Bivand et al., 2013) for each year and, again, using $wind_s$, $wind_l$ and *yday* as predictors and W for spatial weights. For both the non-spatial and autoregressive models we tested for remaining spatial autocorrelation using a Monte Carlo permutation test. In such a test the observed values are randomly assigned to cells after which Moran's I is computed; this procedure is repeated 1000 times (Bivand et al., 2013). The number of times that the actual Moran's I statistic is larger than the Moran's I based on the randomly assigned values, is the permutation test significance level.

2.4.2. Spatial panel error model

Panel data models are useful for modelling changing sediment composition because they allow relationships between the dependent variable and the independent variables to vary across space and time. To account for spatial dependence across cells and temporal change within cells we analysed the dynamics of *Amgs* and *Amud* using spatial panel error models (separate models for *Amgs* and *Amud*) (Kapoor et al., 2007; Millo and Piras, 2012). Heterogeneity across cells can be accounted for by means of fixed effects models and random effects models. The fixed effects model estimates individual intercepts and in the random effects model, the individual effects are modelled in the error term. The objective of our analyses is to make conditional inferences about our sample, i.e. the intertidal area in the Dutch Wadden Sea which has been sampled in its entirety. Elhorst (2014) argues that in cases when data on all spatial units are collected it is questionable whether they can still be considered representative of a

larger population and suggests that in such cases fixed effects models should be specified. Furthermore, the spatial Hausman test, which is developed to discriminate between random and fixed effects models (Mutl and Pfaffermayr, 2011), indicated that fixed effects models were most appropriate in our cases.

The spatial panel fixed effects models contain individual cell effects and year effects. Spatial dependence is modelled within the error term by means of a spatial weights matrix representing the structure of the spatial system. The model reads

$$y = (\iota_T \otimes I_N)\mu + (I_T \otimes \iota_N)\zeta + X\beta + u \quad (1)$$
$$u = \rho(I_T \otimes W_N)u + \epsilon$$

where y represents the $NT \times 1$ vector of the dependent variables $Amgs$ and $Amud$ ($N = 1619$ and $T = 11$). ι_T is a $T \times 1$ vector of ones and I_N is an $N \times N$ identity matrix and μ is the $N \times 1$ vector of time-invariant individual effects which takes into account the individual differences between cells. I_T is a $T \times T$ identity matrix and ι_N is a $N \times 1$ vector of ones and ζ takes into account the year effects; they are treated as fixed effects. X is a $NT \times k$ matrix of independent variables (including intercept) and β is a $k \times 1$ vector containing the estimated coefficients for the independent variables. $\otimes$ is the Kronecker product. u is a spatially autocorrelated composite error term. ρ is the spatial autoregressive parameter. W is the same as above. ϵ is assumed to follow an independent and identical normal distribution with a mean of 0 and standard deviation σ_ϵ.

Data management, preparation and analyses were done with R (R Core Team, 2020; Wickham et al., 2019). For computing Moran's I and Monte Carlo significance testing and estimating simultaneous autoregressive models we used the library *spatialreg* in R which is based on *spdep* (Bivand et al., 2008). The R package *spml* (Millo and Piras, 2012) was used for estimating spatial panel models and for the spatial Hausman test.

3. Results

3.1. Data overview

In the Dutch Wadden Sea the overall means and standard deviations of *mgs* and *mud* of the surface sediment of the intertidal flats are 152 ± 43 μm and $13 \pm 14\%$. The coarsest sediments contain no mud while the finest sediments may contain more than 75% mud. The maps in Fig. 3 show the mean, the standard deviation and the average yearly change for *mgs* and *mud* in the period 2009–2019. Relatively coarse sediments with *mgs* between 200 and 300 μm occur towards the tidal inlets and at the edges of tidal flats near large water bodies, and the fine-grained and muddy sediments are found near the shores and on tidal divides. The most variable locations in terms of the standard deviations of *mgs* and *mud* are located at the edges of intertidal flats, near the shores and at the tidal divides.

The bottom panels in Fig. 3 show the average yearly change in *mgs* and *mud* per cell based on the linear regression analysis. The mean and standard deviation of the regression slopes for *mgs* is 0.20 ± 2.04 μm y^{-1}. The yearly mean change and standard deviation in mud content are $-0.8 \pm 6.5\% y^{-1}$. These results imply that the overall sediment composition has not changed much over the period 2009–2019 but that substantial changes have occurred on the scales of cells. Areas where *mgs* first increased and then decreased, occurred throughout the entire Wadden Sea but these changes were not especially pronounced in specific areas. Similarly, locations at which the mud content first decreased and then increased are evenly spread throughout the region. Maps, frequency distributions and box-plots of yearly *mud* and *mgs* by tidal basin are provided in supplement B.

Fig. 4 presents maps with the yearly anomalies of the median grain size (*Amgs*) and mud content (*Amud*) and Fig. 5 shows the same data in the form of box-plots where observations were grouped on the basis of tidal basin. The highest anomalies are observed in 2014 and 2015. The anomalies are synchronized in the sense that the changes happen similarly throughout the Dutch Wadden Sea.

Table 2
Spatial panel models for yearly changes in median grain size and mud content.

	Parameter	Coefficient	SE	t value	P value
	ρ	0.139	0.016	8.92	0.00
	$yday$	−0.013	0.006	−2.19	0.03
	$wind_s$	0.051	0.042	1.20	0.23
Amgs	$wind_l$	0.401	0.534	0.75	0.45
	R^2	0.044			
	Obs	1619			
	ρ	0.248	0.014	17.26	0.00
	$yday$	−0.00002	0.0002	−0.10	0.92
	$wind_s$	−0.003	0.002	−2.07	0.04
Amud	$wind_l$	−0.064	0.020	−3.20	0.00
	R^2	0.062			
	Obs	1619			

3.2. Nonspatial and spatial autoregressive models

For both *Amgs* and *Amud* there is similarity between the residuals of neigbouring cells resulting in significant spatial autocorrelation in the residuals of the linear regression models. In the linear models, the Moran's I statistics vary between 0.01 and 0.10 (Supplement D). For all linear models, except for *Amgs* in 2019, the permutation significance values were below 0.05. The spatial autocorrelation disappears when it is accounted for by fitting simultaneous autoregressive models. In none of the simultaneous autoregressive models the Moran's I statistic was greater than 0 at a significance level of 0.05. This suggests that a W matrix based on a cutoff distance of 2000 m is adequate for modelling the spatial autocorrelation.

3.3. Spatial panel data models

The estimates for *Amgs* and *Amud* for the spatial panel data models are reported in Table 2. We hypothesized that an increase in the wind speed prior to sampling, on short and longer timescales, would result in coarser sediments. The signs of the $wind_s$ and $wind_l$ coefficients are in line with this hypothesis, i.e. positive for *Amgs* and negative for *Amud*. None of the coefficients in the *Amgs* model are statistically significant at the level 0.05. In the *Amud* model, both the coefficients for $wind_s$ and $wind_l$ are statistically significant at the level of 0.05. The effect of the number of days since June 1 on *Amud* was negative and statistically significant ($p < 0.05$) for *Amgs* but non-significant for *Amud*. This means that during the sampling period between June and October the median grain size decreased. Although the effects of the predictors were in line with our hypotheses, they did not explain much of the variability as indicated by the low R^2 values.

Fig. 6 shows the fixed effects for year for the *Amgs* and *Amud* models. Between 2009 and 2013 the yearly changes in *Amgs* are subtle and in 2014 and 2015 *Amgs* increases substantially. A similar but opposite pattern is observed for *Amud* although here the effect is less pronounced for 2014. For example in 2015, the fixed effect for *Amgs* was 5.0 μm and −0.18 for *Amud;* back-transformation of the fixed effect of −0.18 for Amud in 2015 gives $e^{-0.18} = 0.83$ which implies that in 2015 the effect of the (unobserved) factor caused a reduction of mud content in the intertidal flats of ~17% relative to the mean mud content.

4. Discussion

Because of sea level rise and increasing anthropogenic activities there is an urgent need for a better understanding of sediment dynamics in soft-sediment coastal areas. There are many known and unknown processes operating on different spatial and temporal scales, that influence the sediment grain size distributions in these systems. This makes it challenging to understand and model sediment dynamics, and associated geomorphological and ecological processes. On the basis of

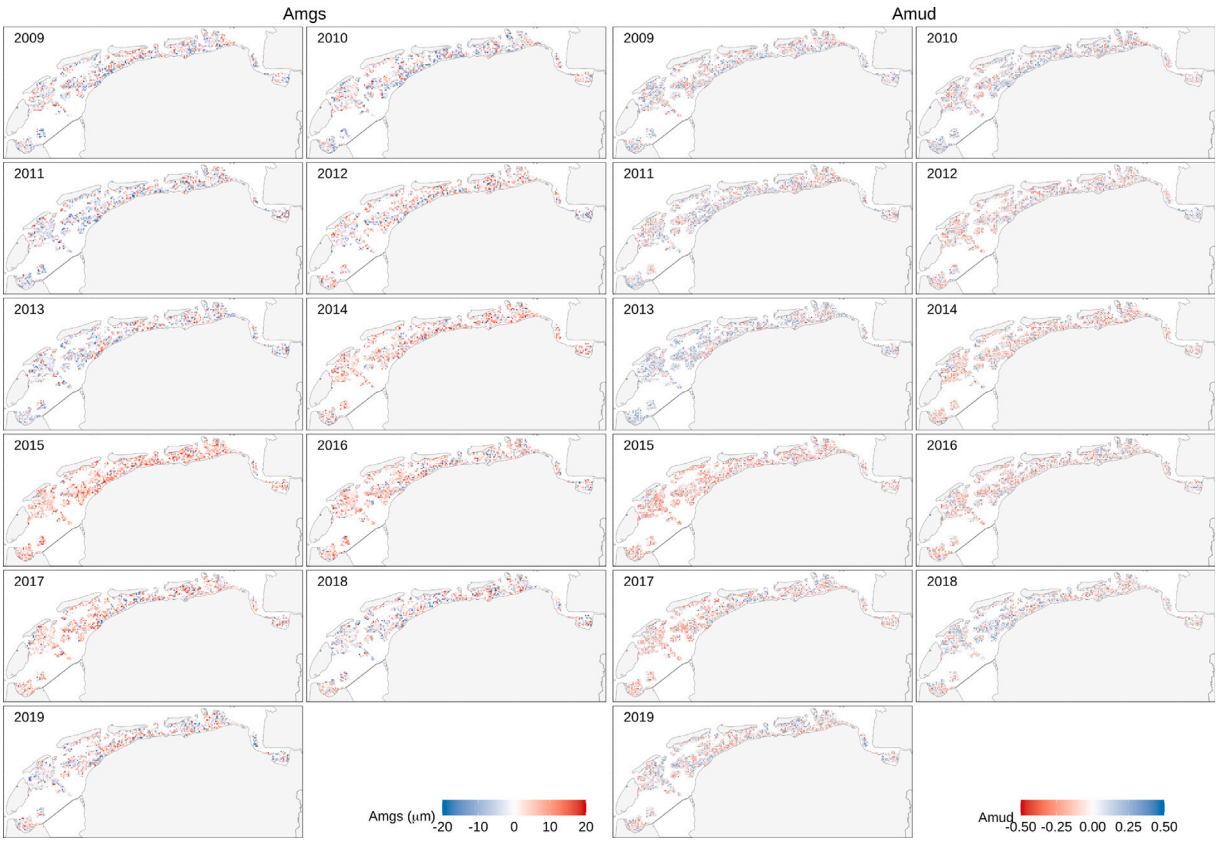

Fig. 4. Yearly anomalies *Amgs* (μm) and *Amud* in the Dutch Wadden Sea.

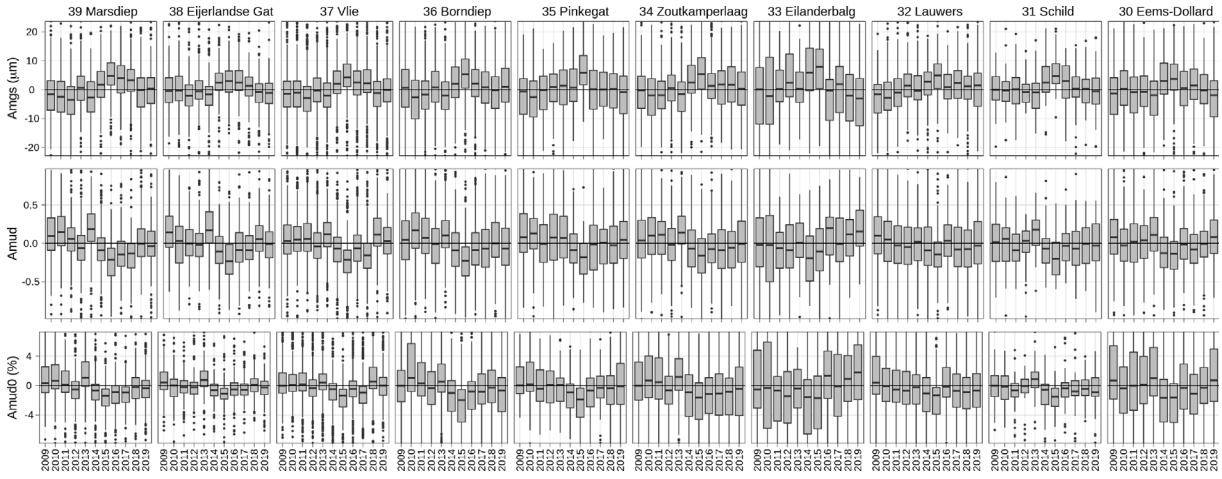

Fig. 5. Boxplots of the yearly anomalies *Amgs, Amud* and *Amud0* by tidal basin. The black horizontal lines represents the median values. The grey boxes represent the first and third quartiles. The whiskers are 1.5 times the distance between the first and third quartile. The black dots are individual datapoints that fall outside the range of the whiskers.

a large number of observations in the period 2009–2019 covering more than 900 km^2, we were able to detect clear spatio-temporal patterns in the sediment composition of the intertidal flats in the Dutch Wadden Sea. We observed relatively high temporal variability of *mgs* and *mud* at the gully edges of tidal flats, near the shores and at tidal divides. The high variability at the edges of intertidal flats is probably the result of forceful erosion and sedimentation processes and changing morphology at the lower intertidal zones (Elias et al., 2012). The high variability near the shores and at the tidal divides can be explained by the fact that sedimentation rates of fine sediments are high at these locations and that mud is easily resuspended (de Jonge and van Beusekom, 1995; Christiansen et al., 2006). Most interesting perhaps was the finding of substantial synchronic large-scale changes in *mgs* and *mud* between years. Our findings are useful in themselves but they also raise new scientific questions and our results can be used to support the improvement of geomorphological models.

We found that over the period 2009–2019 2014 and 2015 were exceptional years in terms of low mud content and large mgs. The finding that the dynamics were synchronized across the entire Dutch Wadden Sea suggests that a large-scale factor was responsible for the changes rather than local disturbances. This finding is in line with the study of Zwarts et al. (2004) who also found synchronized changes in silt concentration between a number of areas in the eastern Dutch Wadden Sea in the period 1975–2000. Zwarts et al. (2004) compiled and

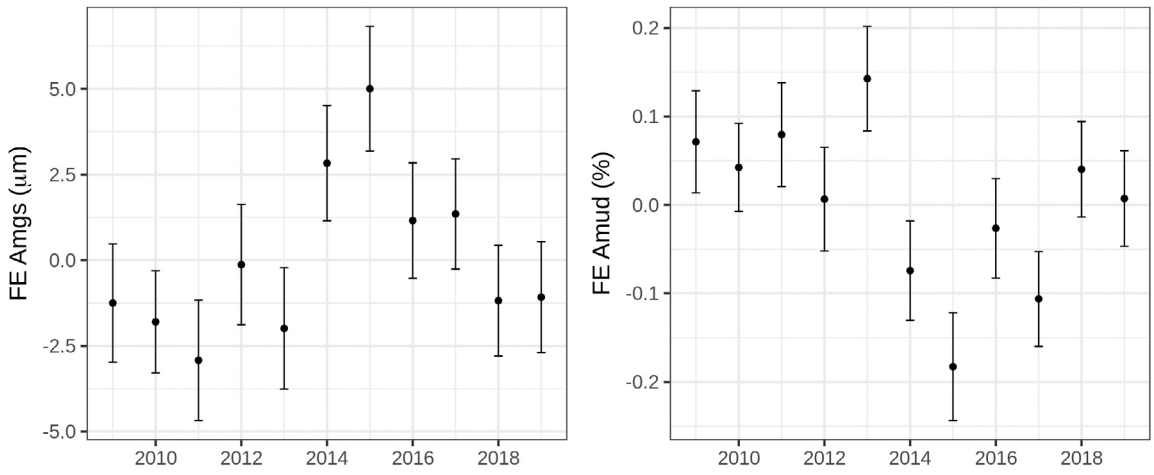

Fig. 6. Estimated fixed effects for year for the *Amgs* and *Amud* models.

harmonized Wadden Sea sediment data from various sources collected during 1950–2000. They observed that at first sight, the intertidal flats had become siltier during this period. However, they note that methodological differences (a.o. time of sampling, depth of samples, grain size distribution measurements) complicate fair comparison. Because methodology strongly affects grain size measurements we did not further compare our data with those of Zwarts et al.

The spatial panel models showed that there was a small effect of the wind conditions prior to sampling on the sediment composition. Particularly, there was a negative effect of winds greater than 5 ms^{-1} two days prior to sampling and a negative effect of winds greater than 8 ms^{-1} over 300 days prior to sampling on *Amud*. The effect of wind on sediment resuspension on intertidal flats has previously been illustrated by means of simulations with hydrodynamic models (Mariotti et al., 2010) and empirically albeit on smaller time and spatial scales (de Jonge and van Beusekom, 1995; Christiansen et al., 2006; Colosimo et al., 2020). Furthermore, it is well-known that wind causes turbulent flow and increases vertical mixing which reduces the deposition rate of suspended sediment (de Vet et al., 2020; Friedrichs, 2011; van Leussen, 1999; Voulgaris and Meyers, 2004). We found no evidence that the wind systematically changed over this period and analyses of long-term wind data do not show systematic change over the past century (van den Hurk et al., 2014). Climate models suggest that in the near future extreme winds from a westerly direction will increase in frequency which, other things equal, may cause coarsening of the sediment.

Our research cannot show what the major cause of the changes in the sediment composition of the tidal flats between years was. There are many processes, operating on varying temporal and spatial scales, that can affect the sediment composition. The finding that the yearly changes were synchronized throughout the Dutch Wadden Sea and that local deviations from this main pattern were not observed, suggests that processes operating on large spatial scales were dominant. Although the yearly deviations in the sediment composition are substantial (the fixed effects of *Amgs* and *Amud* are 5.0 µm and 17% in 2015), there is no clear trend during the period 2009–2019. We do not expect that the differences in the sediment composition would have seriously affected the net sediment dynamics during this period. Our finding is mostly interesting because it points to system-wide cause that still requires identification. We will now make suggestions for further research relating to sea level variations, import of sediment and biotic interactions.

The average rate of sea level rise in the Wadden Sea area was about 1.9 mm y^{-1}during the past 124 years but the year-to-year variability of the sea level is substantial due to weather and the 18.6 year nodal cycle (e.g. Oost et al., 1993; Elias et al., 2012; Vermeersen et al., 2018). Analysis of the morphodynamic evolution of the Dutch Wadden Seay by Elias et al. (2012) shows that import of sand and mud has been more than sufficient to balance sea level rise during the period 1927/1935-2005. Colina Alonso et al. (2021) focused on the separate contributions of sand and mud and showed that during the last two decades sand import into the Western Wadden Sea has stabilized around zero whereas mud import is still ongoing. Even though the import of sediment compensates the long term sea level rise, the year-to-year variability in sea level causes variability in current velocities and constantly brings the geomorphological system in disequilibrium. In the Wadden Sea, increases in water level will decrease the energy dissipation over the subtidal, and increase it over the intertidal. Probably, the increasing bottom shear stress will vary spatially across the intertidal and we expect that the upper intertidal areas will be more strongly affected by erosion than the lower intertidal areas because the relative increase in inundation time, and associated shear, will be larger in the upper intertidal. Another possible cause of the changing sediment composition is variability of the suspended particular matter concentration in the North Sea which is tightly coupled to the Wadden Sea (Herman et al., 2018).

Intertidal ecosystem engineers such as microphytobenthos (benthic microalgae and cyanobacteria) and musselbeds also influence the sediment composition. Microphytobenthos locally reduce the erodability of sediment which leads to finer sediment composition. Musselbeds can reduce the sediment grain size by reducing current velocities and by deposition of nutrient-rich feces and pseudofeces which stimulate the growth of microphytobenthos (Widdows and Brinsley, 2002; van der Zee et al., 2012; Folmer et al., 2014). We especially expect microphytobenthos to have important effects because of its broad spatial distribution on intertidal flats (van der Wal et al., 2010). Although the density of ecosystem engineers varies seasonally (microphytobenthos) or is locally important (musselbeds), an important topic for future research concerns the macro-scale and long-term effects of ecosystem engineers on the sediment.

Understanding sediment dynamics in intertidal systems is challenging but our analyses revealed regularity in the spatial distribution of sediments and in the changes thereof. To improve our understanding of the large number of interacting cause and effect relationships, even longer time series of both sediment data and the physical and biological environment will be required. Furthermore, to be able to capture short-term grain size dynamics and seasonal effects related to e.g. winter storms and accumulation of fine sediment during summer, time series at high temporal resolution are required. For such a purpose, a limited numbers of sampling stations (~100 stations) on the scale of 1–3 km^2 sampled monthly or bi-monthly (or in response to storms and other environmental drivers) would probably suffice. For example, in a study in the Westerschelde estuary Herman et al. (2001) sampled 92

stations on a grid with spacing of ~120 m four times during a period of 10 months. Ideally, this kind of monitoring would be combined with geomorphological simulations where cause and effect relationships are modelled mechanistically. If a geomorphological model is able to simulate the short-term sediment dynamics adequately, such a model can be employed to simulate sediment dynamics on a larger scale and be confronted with large-scale data, as presented in this paper. In addition to longer and temporally denser time series of grain size, it could be useful to also consider the shape and density of the grain (Van Rijn et al., 2007). Spatial panel models are flexible and useful for modelling relationships between the sediment and spatially and temporally varying predictors related to sea level rise, climate change, hydrodynamics, sediment supply and ecological processes.

CRediT authorship contribution statement

Eelke O. Folmer: Designed the study, Prepared the figures, Did the analyses, Spearheaded writing the manuscript, Interpretation of the results, Writing of the manuscript. **Allert I. Bijleveld:** Managed the SIBES monitoring program, Data curation, Interpretation of the results, Writing of the manuscript. **Sander Holthuijsen:** Managed the SIBES monitoring program, Data curation, Interpretation of the results, Writing of the manuscript. **Jaap van der Meer:** Managed the SIBES monitoring program, Interpretation of the results, Writing of the manuscript. **Theunis Piersma:** Managed the SIBES monitoring program, Data curation, Interpretation of the results, Writing of the manuscript. **Henk W. van der Veer:** Managed the SIBES monitoring program, Interpretation of the results, Writing of the manuscript.

Declaration of competing interest

The authors declare that they have no known competing financial interests or personal relationships that could have appeared to influence the work reported in this paper.

Data availability

Data and code are available at the link https://figshare.com/articles/software/Script_and_background_data_for_ECSS_sediment_paper/21997148/1

Acknowledgements

We thank the crew of the RV Navicula, volunteers and colleagues for supporting the SIBES program. We are grateful to Anne Dekinga, Andre Dijkstra, Job ten Horn, Loran Kleine Schaars, Jeroen Kooijman, Anita Koolhaas, Simone Miguel, Luc de Monte, Dennis Mosk, Bianka Rasch, Charlotte Saull, Marten Tacoma, and Evaline van Weerlee for their work in the field and in the laboratory and for managing the SIBES database. We thank Tanya Compton, Katja Philippart, Paolo Stocchi, Peter Herman, Theo Prins and Petra Damsma and an anonymous referee and the non-anonymous referee Job Dronkers for discussion and useful suggestions.

Appendix A. Supplementary data

Supplementary material related to this article can be found online at https://doi.org/10.1016/j.ecss.2023.108308.

References

Beets, D.J., Spek, A.J.F.v.d, 2000. The Holocene evolution of the barrier and the back-barrier basins of Belgium and the Netherlands as a function of late Weichselian morphology, relative sea-level rise and sediment supply. Neth. J. Geosci. 79, 3–16. http://dx.doi.org/10.1017/S0016774600021533.

Bijleveld, A.I., van Gils, J.A., van der Meer, J., Dekinga, A., Kraan, C., van der Veer, H.W., Piersma, T., 2012. Designing a benthic monitoring programme with multiple conflicting objectives. Methods Ecol. Evol. 3, 526–536. http://dx.doi.org/10.1111/j.2041-210X.2012.00192.x.

Bivand, R., Anselin, L., Berke, O., Bernat, A., Carvalho, M., Chun, Y., Dormann, C., Dray, S., Halbersma, R., Lewin-Koh, N., Ma, J., Millo, G., Mueller, W., Ono, H., Peres-Neto, P., Reder, M., Tiefelsdorf, M., Yu, a. D., 2008. spdep: Spatial dependence: Weighting schemes, statistics and models. R package version 0.4-24.

Bivand, R.S., Pebesma, E., Gómez-Rubio, V., 2013. Applied Spatial Data Analysis with R. Use R!, second ed. Springer-Verlag, New York.

Borsje, B.W., van Wesenbeeck, B.K., Dekker, F., Paalvast, P., Bouma, T.J., van Katwijk, M.M., de Vries, M.B., 2011. How ecological engineering can serve in coastal protection. Ecol. Eng. 37, 113–122. http://dx.doi.org/10.1016/j.ecoleng.2010.11.027.

Cahoon, D.R., Hensel, P.F., Spencer, T., Reed, D.J., McKee, K.L., Saintilan, N., 2006. Coastal Wetland Vulnerability to Relative Sea-Level Rise: Wetland Elevation Trends and Process Controls. In: Verhoeven, J.T.A., Beltman, B., Bobbink, R., Whigham, D.F. (Eds.), Wetlands and Natural Resource Management. In: Ecological Studies, Springer Berlin Heidelberg, Berlin, Heidelberg, pp. 271–292. http://dx.doi.org/10.1007/978-3-540-33187-2_12, URL https://doi.org/10.1007/978-3-540-33187-2-12.

Christiansen, C., Vølund, L.C., Bartholdy, J., 2006. Wind influence on tidal flat sediment dynamics: Field investigations in the Ho Bugt, Danish Wadden sea. Mar. Geol. 235, 75–86. http://dx.doi.org/10.1016/j.margeo.2006.10.006, URL https://linkinghub.elsevier.com/retrieve/pii/S0025322706002593.

Colina Alonso, A., van Maren, D.S., Elias, E.P.L., Holthuijsen, S.J., Wang, Z.B., 2021. The contribution of sand and mud to infilling of tidal basins in response to a closure dam. Mar. Geol. 439, 106544. http://dx.doi.org/10.1016/j.margeo.2021.106544.

Colosimo, I., d. Vet, P.L.M., van Maren, D.S., Reniers, A.J.H.M., Winterwerp, J.C., van Prooijen, B.C., 2020. The impact of wind on flow and sediment transport over intertidal flats. J. Mar. Sci. Eng. 8 (910), http://dx.doi.org/10.3390/jmse8110910.number:11.

Compton, T.J., Holthuijsen, S., Koolhaas, A., Dekinga, A., Horn, J.ten., Smith, J., Galama, Y., Brugge, M., van der Wal, D., van der Meer, J., van der Veer, H.W., Piersma, T., 2013a. Distinctly variable mudscapes: Distribution gradients of intertidal macrofauna across the Dutch Wadden Sea. J. Sea Res. 82, 103–116. http://dx.doi.org/10.1016/j.seares.2013.02.002.

Compton, T.J., Meer, J.van der., Holthuijsen, S., Koolhaas, A., Dekinga, A., ten Horn, J., Klunder, L., McSweeney, N., Brugge, M., van der Veer, H.W., 2013b. Synoptic Intertidal Benthic Surveys across the Dutch wadden sea 2008 to 2011. Technical Report NIOZ 2013-1, NIOZ, Texel.

de Jonge, V.N., van Beusekom, J.E.E., 1995. Wind- and tide-induced resuspension of sediment and microphytobenthos from tidal flats in the Ems estuary. Limnol. Oceanogr. 40, 776–778. http://dx.doi.org/10.4319/lo.1995.40.4.0776.

de Vet, P.L.M., van Prooijen, B.C., Colosimo, I., Steiner, N., Ysebaert, T., Herman, P.M.J., Wang, Z.B., 2020. Variations in storm-induced bed level dynamics across intertidal flats. Sci. Rep. 10, 12877. http://dx.doi.org/10.1038/s41598-020-69444-7.

Dijkema, K.S., Reineck, H.E., Wolff, W.J., 1980. Geomorphology of the Wadden Sea Area. In: volume no. 1. of *Report (Wadden Sea Working Group)*.

Donker, J.J.A., 2015. Hydrodynamic processes and the stability of intertidal mussel beds in the dutch Wadden Sea. In: Utrecht Studies in Earth Sciences.

Eisma, D., 1986. Flocculation and de-flocculation of suspended matter in estuaries. Neth. J. Sea Res. 20, 183–199. http://dx.doi.org/10.1016/0077-7579(86)90041-4.

Elhorst, J.P., 2014. Spatial Panel Data Models. In: Spatial Econometrics. In: SpringerBriefs in Regional Science, Springer, Berlin, Heidelberg, pp. 37–93.

Elias, E.P.L., Spek, Wang, Z.B., Ronde, J.d., 2012. Morphodynamic development and sediment budget of the Dutch Wadden Sea over the last century. Neth. J. Geosci. 91, 293–310. http://dx.doi.org/10.1017/S0016774600000457.

Folmer, E.O., Drent, J., Troost, K., Büttger, N., Jansen, J., Va. Stralen, M., Millat, G., Herlyn, M., Philippart, C.J.M., 2014. Large-scale spatial dynamics of intertidal mussel (*Mytilus edulis L.*) bed coverage in the German and Dutch Wadden Sea. Ecosystems 17, 550–566. http://dx.doi.org/10.1007/s10021-013-9742-4.

Folmer, E.O., Van Beusekom, J.E.E., Dolch, T., Gräwe, M.M., Kolbe, K., Philippart, C.J.M., 2016. Consensus forecasting of intertidal seagrass habitat in the Wadden Sea. J. Appl. Ecol. 53, 1800–1813. http://dx.doi.org/10.1111/1365-2664.12681.

Friedrichs, C.T., 2011. 3.06 - Tidal Flat Morphodynamics: A Synthesis. In: Wolanski, E., McLusky, D. (Eds.), Treatise on Estuarine and Coastal Science. Academic Press, Waltham, pp. 137–170. http://dx.doi.org/10.1016/B978-0-12-374711-2.00307-7.

Grabowski, R.C., Droppo, I.G., Wharton, G., 2011. Erodibility of cohesive sediment: The importance of sediment properties. Earth-Sci. Rev. 105, 101–120. http://dx.doi.org/10.1016/j.earscirev.2011.01.008.

Gräwe U. Flöser, T., Duran-Matute, M., Badewien, T.H., Schulz, E., Burchard, H., 2016. A numerical model for the entire Wadden Sea: Skill assessment and analysis of hydrodynamics. J. Geophys. Res.: Oceans 121, 5231–5251. http://dx.doi.org/10.1002/2016JC011655.

Herman, P.M.J., van Kessel, T., Vroom, J., Dankers, P., Cleveringa, J., de Vries, B., Villars, N., 2018. Mud Dynamics in the Wadden Sea - Towards a Conceptual Model. Technical Report, Deltares.

Herman, P.M., Middelburg, J.J., Heip, C.H., 2001. Benthic community structure and sediment processes on an intertidal flat: Results from the ECOFLAT project. Cont. Shelf Res. 21, 2055–2071. http://dx.doi.org/10.1016/S0278-4343(01)00042-5.

Holgate, S.J., Matthews, A., Woodworth, P.L., Rickards, L.J., Tamisiea, M.E., Bradshaw, E., Foden, P.R., Gordon, K.M., Jevrejeva, S., Pugh, J., 2013. New Data Systems and Products at the Permanent Service for Mean Sea Level. J. Coast. Res. 29, 493–504. http://dx.doi.org/10.2112/JCOASTRES-D-12-00175.1, URL https://bioone.org/journals/journal-of-coastal-research/volume-29/issue-3/JCOASTRES-D-12-00175.1/New-Data-Systems-and-Products-at-the-Permanent-Service-for/10.2112/JCOASTRES-D-12-00175.1.full.

Janssen-Stelder, B., 2000. The effect of different hydrodynamic conditions on the morphodynamics of a tidal mudflat in the Dutch Wadden Sea. Cont. Shelf Res. 20, 1461–1478. http://dx.doi.org/10.1016/S0278-4343(00)00032-7.

Kabat, P., Jacobs, C.M.J., Hutjes, R.W.A., Hazeleger, W., Engelmoer, M., 2009. Klimaatverandering En Het Waddengebied. 2009-06. De Waddenacademie KNAW..

Kamps, L., 1962. Mud Distribution and Land Reclamation in the Eastern Wadden Shallows. Technical Report 4, Rijkswaterstaat. The Hague.

Kapoor, M., Kelejian, H.H., Prucha, I.R., 2007. Panel data models with spatially correlated error components. J. Econometrics 140, 97–130. http://dx.doi.org/10.1016/j.jeconom.2006.09.004.

Kirwan, M.L., Megonigal, J.P., 2013. Tidal wetland stability in the face of human impacts and sea-level rise. Nature 504, 53–60. http://dx.doi.org/10.1038/nature12856.

Le Hir, P., Roberts, W., Cazaillet, O., Christie, M., Bassoullet, P., Bacher, C., 2000. Characterization of intertidal flat hydrodynamics. Cont. Shelf Res. 20, 1433–1459. http://dx.doi.org/10.1016/S0278-4343(00)00031-5.

Malvarez, G.C., Cooper, J.a.G., Jackson, D.W.T., 2001. Relationships between wave-induced currents and sediment grain size on a sandy tidal-flat. J. Sediment. Res. 71, 705–712. http://dx.doi.org/10.1306/2DC40961-0E47-11D7-8643000102C1865D.

Mariotti, G., Fagherazzi, S., Wiberg, P.L., McGlathery, K.J., Carniello, L., Defina, A., 2010. Influence of storm surges and sea level on shallow tidal basin erosive processes. J. Geophys. Res.: Oceans 115, C11012. http://dx.doi.org/10.1029/2009JC005892.

Millo, G., Piras, G., 2012. splm: Spatial panel data models in R. J. Stat. Softw. 47, 1–38.

Montserrat, F., Colen, C.V., Degraer, S., Ysebaert, T., Herman, P.M.J., 2008. Benthic community-mediated sediment dynamics. Mar. Ecol. Prog. Ser. 372, 43–59. http://dx.doi.org/10.3354/meps07769.

Mullan Crain, C., Bertness, M.D., 2006. Ecosystem engineering across environmental gradients: Implications for conservation and management. BioScience 56, 211. http://dx.doi.org/10.1641/0006-3568(2006)056[0211:EEAEGI]2.0.CO;2.

Mutl, J., Pfaffermayr, M., 2011. The Hausman test in a Cliff and Ord panel model. Econom. J. 14, 48–76. http://dx.doi.org/10.1111/j.1368-423X.2010.00325.x.

Oost, A.P., 1995. Sedimentological implications of morphodynamic changes in the ebb-tidal delta, the inlet and the drainage basin of the zoutkamperlaag tidal inlet (Dutch wadden sea), induced by a sudden decrease in the tidal prism. In: Flemming, B.W., Bartholomä, A. (Eds.), Tidal Signatures in Modern and Ancient Sediments. John Wiley & Sons, Ltd, pp. 101–119. http://dx.doi.org/10.1002/9781444304138.ch7.

Oost, A.P., de Haas, H., Ijnsen, F., van den Boogert, J.M., de Boer, P.L., 1993. The 18.6 yr nodal cycle and its impact on tidal sedimentation. Sediment. Geol. 87, 1–11. http://dx.doi.org/10.1016/0037-0738(93)90032-Z.

Paterson, D., Black, K., 1999. Water flow, sediment dynamics and benthic biology. In: Estuaries, Vol. 29. Academic Press, pp. 155–193.

R Core Team, 2020. R: A Language and Environment for Statistical Computing. R Foundation for Statistical Computing, Vienna, Austria. URL https://www.R-project.org/.

Reise, K., Baptist, M., Burbridge, P., Dankers, N., Fischer, L., Flemming, B., Oost, A., 2010. The Wadden Sea 2010 - A Universally Outstanding Tidal Wetland. Synthesis Report 29, CWSS, Wilhelmshaven, Germany.

Roberts, W., Le Hir, P., Whitehouse, R.J.S., 2000. Investigation using simple mathematical models of the effect of tidal currents and waves on the profile shape of intertidal mudflats. Cont. Shelf Res. 20, 1079–1097. http://dx.doi.org/10.1016/S0278-4343(00)00013-3.

Schlüter, M., Jerosch, K., 2009. Digital Atlas of the North Sea. Alfred Wegener Institute for Polar and Marine Research et al.

Temmerman, S., Meire, P., Bouma, T.J., Herman, P.M.J., Ysebaert, T., De Vriend, H.J., 2013. Ecosystem-based coastal defence in the face of global change. Nature 504, 79–83. http://dx.doi.org/10.1038/nature12859.

van den Hurk, B., Siegmund, P., Attema, J., Bakker, A., Beersma, J., Bessembinder, J., Boers, R., Brandsma, T., van den Brink, H., Drijfhout, S., Eskes, H., Haarsma, R., Hazeleger, W., Jilderda, R., Katsman, C., Lenderink, G., Loriaux, J., van Meijgaard, E., van Noije, T., van Oldenborgh, G.J., Selten, F., Siebsma, P., Sterl, A., de Vries, H., van Weele, M., d. Winter, R., van Zadelhoff, G.J., 2014. KNMI'14: Climate Change Scenarios for the 21st Century - a Netherlands Perspective.

van der Wal, D., Wielemaker-van den Dool, A., Herman, P.M.J., 2010. Spatial synchrony in intertidal benthic algal biomass in temperate coastal and estuarine ecosystems. Ecosystems 13, 338–351. http://dx.doi.org/10.1007/s10021-010-9322-9.

van der Zee, E., van der Heide, T., Donadi, S., Eklöf, B., Olff, H., van der Veer, H., Piersma, T., 2012. Spatially extended habitat modification by intertidal reef-building bivalves has implications for consumer-resource interactions. Ecosystems 15, 664–673. http://dx.doi.org/10.1007/s10021-012-9538-y.

Van Goor, M.A., Zitman, T.J., Wang, Z.B., Stive, M.J.F., 2003. Impact of sea-level rise on the morphological equilibrium state of tidal inlets. Mar. Geol. 202, 211–227. http://dx.doi.org/10.1016/S0025-3227(03)00262-7.

van Leussen, W., 1999. The variability of settling velocities of suspended fine-grained sediment in the Ems estuary. J. Sea Res. 41, 109–118. http://dx.doi.org/10.1016/S1385-1101(98)00046-X.

Van Rijn, L., Walstra, D., Va. Ormondt, M., 2007. Unified view of sediment transport by currents and waves. IV: Application of morphodynamic model. J. Hydraul. Eng. 133, 776–793.

van Straaten, L.M.J.U., Kuenen, P.H., 1958. Tidal action as a cause of clay accumulation. J. Sediment. Res. 28, 406–413. http://dx.doi.org/10.1306/74D70826-2B21-11D7-8648000102C1865D.

Vermeersen, B.L.A., Slangen, A.B.A., Gerkema, T., Baart, F., Cohen, K.M., Dangendorf, S., Duran-Matute, M., Frederikse, T., Grinsted, A., Hijma, M.P., Jevrejeva, S., Kiden, P., Kleinherenbrink, M., Meijles, E.W., Palmer, M.D., Rietbroek, R., Riva, R.E.M., Schulz, E., Slobbe, D.C., Simpson, M.J.R., Sterlini, P., Stocchi, P., Wal, R.S.W.v.d., Wegen, M.v.d., 2018. Sea-level change in the Dutch Wadden Sea. Neth. J. Geosci. 97, 79–127. http://dx.doi.org/10.1017/njg.2018.7, publisher: Cambridge University Press.

Voulgaris, G., Meyers, S.T., 2004. Temporal variability of hydrodynamics, sediment concentration and sediment settling velocity in a tidal creek. Cont. Shelf Res. 24, 1659–1683. http://dx.doi.org/10.1016/j.csr.2004.05.006.

Wang, Z.B., Hoekstra, P., Burchard, H., Ridderinkhof, H., D. Swart, H.E., Stive, M.J.F., 2012. Morphodynamics of the Wadden Sea and its barrier island system. Ocean Coast. Manag. 68, 39–57. http://dx.doi.org/10.1016/j.ocecoaman.2011.12.022.

Wickham, H., Averick, M., Bryan, J., Chang, W., McGowan, L.D., François, G., Hayes, A., Henry, L., Hester, J., Kuhn, M., Pedersen, T.L., Miller, E., Bache, S.M., Müller, J., Robinson, D., Seidel, D.P., Spinu, V., Takahashi, K., Vaughan, D., Wilke, C., Woo, K., Yutani, H., 2019. Welcome to the tidyverse. J. Open Source Softw. 4 (1686), http://dx.doi.org/10.21105/joss.01686.

Widdows, J., Blauw, A., Heip, C.H.R., Herman, P.M.J., Lucas, C.H., Middelburg, J.J., Schmidt, S., Brinsley, M.D., Twisk, F., Verbeek, H., 2004. Role of physical and biological processes in sediment dynamics of a tidal flat in Westerschelde Estuary, SW Netherlands. Mar. Ecol. Prog. Ser. 274, 41–56.

Widdows, J., Brinsley, M., 2002. Impact of biotic and abiotic processes on sediment dynamics and the consequences to the structure and functioning of the intertidal zone. J. Sea Res. 48, 143–156. http://dx.doi.org/10.1016/S1385-1101(02)00148-X.

Yang, S.L., Fan, J.Q., Shi, B.W., Bouma, T.J., Xu, K.H., Yang, H.F., Zhang, S.S., Zhu, Q., Shi, X.F., 2019. Remote impacts of typhoons on the hydrodynamics, sediment transport and bed stability of an intertidal wetland in the Yangtze Delta. J. Hydrol. 575, 755–766. http://dx.doi.org/10.1016/j.jhydrol.2019.05.077.

Zwarts, L., Dubbeldam, W., Van den Heuvel, H., Van de Laar, E., Menke, U., Hazelhoff, L., Smit, C.J., 2004. Bodemgesteldheid En Mechanische Kokkelvisserij in de Waddenzee. Technical Report 2004.028, RIZA, Lelystad.